Template-Assembled Triple-Helical Peptide Molecules: Mimicry of Collagen by Molecular Architecture and Integrin-Specific Cell Adhesion†

Shih Tak Khew‡ and Yen Wah Tong*,‡,§

Department of Chemical & Biomolecular Engineering, National University of Singapore, and Division of Bioengineering, National University of Singapore, 21 Lower Kent Ridge Road, Singapore 119077

Received October 9, 2007

ABSTRACT: Most proteins fold into specific structures to exert their biological functions, and therefore the creation of protein-like molecular architecture is a fundamental prerequisite toward realizing a novel biologically active protein-like biomaterial. To do this with an artificial collagen, we have engineered a peptide template characterized by its collagen-like primary structure composed of Gly-Phe-Gly-Glu-Glu-Gly sequence to assemble $(Pro\text{-}Hyp\text{-}Gly)_n$ ($n = 3$ and 5) into triple-helical conformations that resemble the native structure of collagen. The peptide template has three carboxyl groups connected to the N-termini of three collagen peptides. The coupling was accomplished by a simple and direct branching protocol without complex strategies. A series of biophysical studies, including melting curve analyses and CD and NMR spectroscopy, demonstrated the presence of stable triple-helical conformation in the template-assembled $(Pro\text{-}Hyp\text{-}Gly)_3$ and $(Pro\text{-}Hyp\text{-}Gly)_5$ solution. Conversely, nontemplated peptides showed no evidence of assembly of triple-helical structure. A cell binding sequence (Gly-Phe-Hyp-Gly-Glu-Arg) derived from the collagen α_1(I) chain was incorporated to mimic the integrin-specific cell adhesion of collagen. Cell adhesion and inhibition assays and immunofluorescence staining revealed a correlation of triple-helical conformation with cellular recognition of collagen mimetics in an integrin-specific way. This study offers a robust strategy for engineering native-like peptide-based biomaterials, fully composed of only amino acids, by maintaining protein conformation integrity and biological activity.

Most natural proteins fold into a well-defined structure to implement their biological functions. Therefore, the creation of protein-like molecular architecture is the fundamental prerequisite in realizing a novel biologically active protein-like biomaterial. One protein that is of wide interest to many scientists is collagen, which is the principal constituent of extracellular matrices (ECM) in the body. It can be distinguished from other proteins by its unique triple-helical structure composed of three left-handed poly(proline-II)-like chains, staggered by one peptide residue from each other, intertwined into a right-handed triple helix (*1*, *2*). This assembly is a direct consequence of its unique primary structure composed of repetitive Xxx-Yyy-Gly triplets, where X and Y amino acid residues are predominantly Pro and Hyp, respectively. Mimicry of collagen structure has been achieved by using synthetic polypeptides composed of Pro-Pro-Gly or Pro-Hyp-Gly repeat units (*3*−*6*). Various strategies have been employed to realize collagen-like triple-helical structure. Hartgerink and co-workers have recently demonstrated the capability of intermolecular electrostatic interactions to direct self-assembly of heterotrimeric collagen triple helices (*7*). Self-assembly of short collagen peptides into triple helices (*8*) and collagen-like fibrils (*9*), which also mimicked collagen's biological function, has also been accomplished previously. Furthermore, Yu and co-workers demonstrated that the stability of $(Pro\text{-}Hyp\text{-}Gly)_n$ can be significantly improved by modifying the N-termini with hydrophobic compounds such as 5-carboxyfluorescein (*10*). Short collagen peptides can be formed into triple-helical conformation by attaching them onto gold nanoparticles (*11*). In these works, such collagen-mimetic peptides have been used to bind to partially denatured collagen (*10*, *11*). Additionally, Kotch and Raines have recently reported the synthesis of short collagen fragments being held in a staggered array by disulfide bonds and self-assembled into fibrils that resemble natural collagen (*12*). Head-to-tail peptide polymerization utilizing N-cysteine and C-thioester groups has also been performed to achieve collagen-like nanofibers (*13*). On the other hand, to reinforce the intramolecular folding and stabilize the triple-helical conformations of these collagen-like peptides, templates such as lysine dimer (*14*−*18*), glutamate dimer (*19*), 1,2,3-propanetricarboxylic acid (*20*), Kemp triacid (KTA) (*21*, *22*), tris(2-aminoethyl)amine (*23*), and cyclopropane (*24*), or a built-in cysteine-knot (*25*, *26*), have been added into the design of collagen structures. However, the incorporation of the amino acid-based templates such as dilysine and cysteine-knot to assemble collagen peptides poses a number of challenging problems that are usually not encountered in the stepwise synthesis of linear peptides and often required a carefully designed and complex synthesis strategy (*17*−*19*, *26*). Even though many templates have been used to assemble collagen peptides, few have reported the design of a fully amino acid-based collagen mimics and the potential of a longer N-terminal peptide template of collagen-like primary sequence as a carrier for additional bioactive sequences at its extension.

† This work was supported by the National University of Singapore under the grant number R279000168112.

* Corresponding author. E-mail: chetyw@nus.edu.sg. Tel: (+65) 6516-8467. Fax: (+65) 6779-1936.

‡ Department of Chemical & Biomolecular Engineering.

§ Division of Bioengineering.

10.1021/bi702018v CCC: $40.75
Published on Web 12/22/2007

Table 1: Melting Point Temperature (T_m) of the PT-Assembled Collagen Peptides and Their Nontemplated Counterparts[a]

protein/peptides	sequence[b]	T_m (°C)
PT-CP1	(GFGEEG)≡[G-$(POG)_5$]$_3$	59
PT-CP2	(GFGEEG)≡[G-$(POG)_3$]$_3$	30
PT-CP3	(GFGEEG)≡[GG-GPO**GFOGER**GPO-GG]$_3$	20
PT-CP4	(GFGEEG)≡[G-$(GPO)_3$**GFOGER**$(GPO)_3$-G]$_3$	44
CP1	$(POG)_5$	no transition
CP2	$(POG)_3$	no transition
CP3	GPO**GFOGER**GPO	no transition
CP4	$(GPO)_3$**GFOGER**$(GPO)_3$	25
(Pro-Pro-Gly)$_3$	$(PPG)_3$	no transition
(Pro-Hyp-Gly)$_{10}$	$(POG)_{10}$	60
collagen	calf-skin collagen	37

[a] Shown here is the T_m of each peptide as determined by the temperature-dependent UV absorbance measurement at 225 nm. Cell recognition Site (GFOGER) corresponding to residues 502−507 of the collagen α_1 (I) is shown in bold. Each GFGEEG peptide template (PT) contains three carboxylic arms at Its C-terminus for covalent coupling to the N-terminus of the collagen peptides. [b] Standard one-letter code is used to express amino acid sequences, except where noted. O is used to represent hydroxyproline residue.

Integrin-mediated cell adhesion to ECM proteins is known to be crucial for biological processes such as embryogenesis, homeostasis, and tissue remodeling and healing (*27*, *28*). Several regions within the triple-helical domain of collagen have been found to function as cellular recognition binding sites (*29*−*33*). Recent studies have identified the Gly-Phe-Hyp-Gly-Glu-Arg (GFOGER) hexapeptide, derived from residues 502−507 of collagen α_1 (I), as one major cell binding site within type I collagen (*29*, *30*). The triple-helical peptides supplemented with GFOGER was used to engineer bioadhesive surface (*34*, *35*). In this study, this integrin-specific GFOGER cell recognition sequence was also incorporated into the collagen peptides to serve as an integrin-specific adhesion site.

This paper describes the synthesis of a peptide template that is only constituted by amino acids to assemble collagen peptides of different sequences (Table 1) through a simple and direct branching protocol without complex strategies, to study the requirements of collagen-cell interactions in terms of triple-helical molecular architecture together with a cell recognition sequence. The conformational characteristic of the PT[1]-assembled structures was assessed by a series of melting curve analyses and circular dichroism (CD) and nuclear magnetic resonance (NMR) spectroscopy. The peptides were examined for their ability to support cell adhesion in an integrin-specific way by cell adhesion and competition inhibition assays and immunofluorescence staining. The significance of both the triple-helical molecular architecture and specific cell binding site was investigated. This study offers a robust strategy for future attempts to engineer native-like protein biomaterials by maintaining the integrity of protein conformation and its biological activity.

MATERIALS AND METHODS

Materials. All peptide synthesis chemicals and solvents were of analytic reagent grade or better and were purchased from Novabiochem (San Diego, CA) except where noted. All amino acids were of L-configuration and purchased from Novabiochem. Chemical solvents were purchased from Sigma-Aldrich (St. Louis, MO) unless otherwise stated. Acetonitrile (HPLC grade) was purchased from Merck (Darmstadt, Germany).

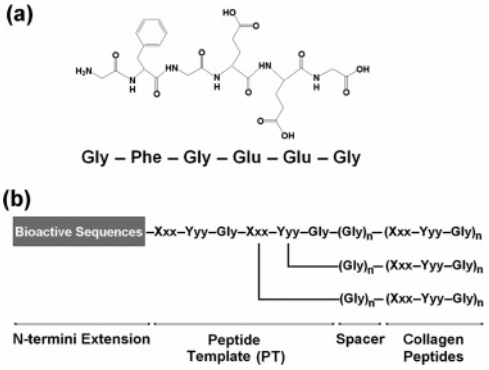

FIGURE 1: Molecular structure of the peptide template (PT) and the PT-assembled collagen-mimetic peptides. (a) Molecular structure of the GFGEEG peptide template. The C-terminus of the template contains three carboxyl groups, each of which can be linked to a strand of collagen peptide to facilitate the interactions of the three peptide chains to form the triple helical conformation. The PT has a primary structure of repeating Xxx-Yyy-Gly triplets that is similar to that of collagen. (b) The PT-assembled collagen peptide. It is a fully amino acid-based collagen analogue, consistent with the native protein, with collagen-like primary and tertiary structure, which also allows incorporation of collagen cell binding sequences within the collagen peptide sequences as well as insertion of additional functional sequences at the N-termini extension of the template.

Synthesis of Fmoc-Protected GFGEEG Template. Fmoc-GFGEEG hexapeptide (Figure 1) was synthesized in-house on an automated Multipep peptide synthesizer (Intavis, Cologne, Germany). The peptide was assembled on Fmoc-Gly-Wang resin (substitution level = 0.66 mmol/g resin) at a 50 μmol scale. Stepwise couplings of amino acids were accomplished using a double coupling method with 5-fold excesses of amino acids, equivalent activator reagents, 2-(1*H*-benzotriazol-1-yl)-1,1,3,3-tetramethyluronium hexafluorophosphate (HBTU) (Advanced Chemtech, Louisville, KY), and *N*-hydroxybenzotriazole (HOBt) (Advanced Chemtech), and two equivalents of base, *N*-methylmorpholine (NMM). Each coupling reaction was allowed to proceed for 0.5 h at room temperature. All Fmoc-protected amino acids and activators were dissolved in dimethylformamide (DMF), except where noted, to saturation. Fmoc-Phe was dissolved in 1-methyl-2-pyrrolidone (NMP). The saturation concentration of Fmoc-amino acids in DMF or NMP is 0.6 M while

[1] Abbreviations: PT, peptide template; CP, collagen peptide; BSA, bovine serum albumin; NMR, nuclear magnetic resonance; CD, circular dichroism; UV, ultraviolet; MALDI-TOF MS, matrix-assisted laser desorption/ionization time of flight mass spectroscopy; HPLC, high performance liquid chromatography.

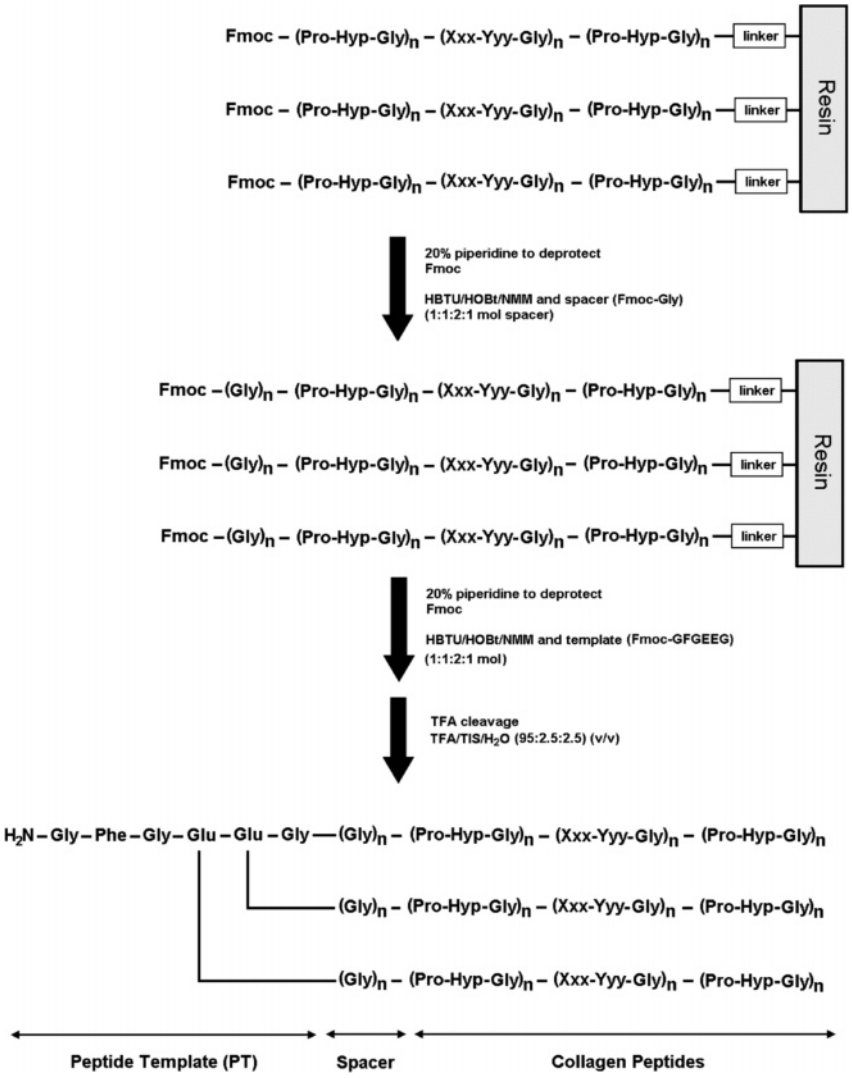

FIGURE 2: Synthesis of the PT-assembled collagen peptides. The collagen peptides of repeating Xxx-Yyy-Gly sequences are synthesized and coupled to the template through a spacer by a simple Fmoc-solid-phase peptide synthesis method.

the saturation concentrations of HBTU and HOBt in DMF are 0.6 and 2.2 M, respectively. NMM was prepared in DMF at 45% (v/v) concentration. The removal of Fmoc was accomplished by using 20% (v/v) piperidine in dimethylformamide (DMF) for 15 min twice. The resin was washed four times with DMF. Cycles of deprotection, washing, double couplings, and washing were repeated until the desired sequence was achieved. The Fmoc protection group at the N-terminus of the peptide was not cleaved. The product was washed with dichloromethane (DCM) twice and vacuum-dried prior to cleavage from the resin using a cocktail solution composed of 95% trifluoroacetic acid (TFA), 2.5% deionized water, and 2.5% triisopropylsilane (TIS) (v/v). The reaction was allowed to proceed for 3 h with occasional shaking. The cleavage solution was added to cold methyl *tert*-butyl ether dropwise to induce precipitation of the peptide. The precipitate was collected by centrifugation and was washed three times with excess of cold ether to remove any residual scavengers. The final precipitate was redissolved and lyophilized.

Synthesis of Collagen Peptides. Collagen peptides (CP1, CP2, CP3, and CP4) as shown in Table 1 were synthesized as described above. The Fmoc protection group at the N-terminus was removed by 20% (v/v) piperidine in DMF prior to the cleavage. The crude peptide was purified on an Agilent 1100 semipreparative HPLC (Santa Clara, CA) equipped with an Agilent Zorbax 300SB-C18 reverse phase (RP) column (5 μm particle size, 300 Å pore size, 25 $\times$ 1.0 cm) using a linear gradient of buffer A (0.1% TFA in water) and buffer B (0.1% TFA in acetonitrile) (10% B to 45% B in 30 min) at a total flow rate of 2.5 mL/min. Detection was set at 215 nm. Analytical HPLC was performed on an Agilent Zorbax 300SB-C18 RP column (5 μm particle size, 300 Å pore size, 25 $\times$ 0.46 cm) at conditions similar to the preparative HPLC except where noted. The total flow rate was 1 mL/min. The purity of all peptides was greater than 95% by analytical RP-HPLC. The mass of the peptides was checked by matrix-assisted laser desorption/ionization time-of-flight mass spectroscopy (MALDI-TOF MS) on a Bruker AutoFlex II MALDI-TOF MS (Bruker, Bremen, Germany).

Synthesis of Peptide Template-Assembled Collagen Peptides. The PT-assembled collagen peptides (PT-CP1, PT-CP2, PT-CP3, and PT-CP4) as shown in Table 1 were synthesized using the Fmoc solid-phase peptide synthesis method (Figure 2). The collagen peptides (CP1, CP2, CP3, and CP4) were first synthesized on the resin (50 μmol based on resin substitution level) as described above. The Fmoc protection group at the N-terminus of the peptide-resin was

removed by 20% (v/v) piperidine in DMF prior to the coupling to the peptide template manually. The resin was washed four times with excess of DMF. Fmoc-GFGEEG (8 μmol) was dissolved in DMF to saturation (0.3 M) and added to the reaction vessel together with 1 equiv of HBTU and HOBt and 2 equiv of NMM, with respect to the carboxylic arms on the peptide template. The coupling of the peptide template to the N-termini of the peptide sequence proceeded for 6 h at room temperature with occasional shaking. The Fmoc protection group was removed as described above. The resin was washed with DMF and DCM twice and vacuum-dried overnight. The cleavage was done as described. Preparative HPLC was performed to give products of purity greater than 85% as given by the analytical HPLC. The mass of the products was examined using MALDI-TOF MS.

MALDI-TOF Mass Spectroscopy. Samples were dissolved in ultrapure water at about 1 μg/mL. The matrix, α-cyano-4-hydroxycinnamic acid (Sigma-Aldrich), was dissolved in acetonitrile/water (50:50 v/v) containing 0.1% TFA to saturation. Equal volumes (0.5 μL) of sample and matrix were mixed thoroughly, spotted on the MTP384 matt steel target plate (Bruker), and air-dried. Data was acquired using reflector detector operating at voltage 1614 V, low laser intensity, and 50 shots per acquisition. Matrix suppression was activated to suppress the matrix signal below 800 m/z.

CD Spectroscopy. CD measurements were performed on a Jasco Model J-810 spectropolarimeter (Jasco, Great Dunmow, Essex, UK) using a quartz cylindrical cuvette (Hellma, Müllheim, Germany) with a path length of 0.1 mm. The cuvette was filled with 150 μL of samples for each measurement. The CD spectra were obtained by continuous wavelength scans (average of three scans) from 260 to 180 nm at a scan speed of 50 nm/min. All samples were dissolved in ultrapure water, unless otherwise stated, and stored at 4 °C for at least 7 days prior to the test to allow for proper equilibration of triple-helical conformation. The samples were equilibrated for at least 1 h at the desired temperature before the CD spectrum was acquired.

Melting Studies. The temperature-dependent UV absorbance of the peptides was measured on a Cary 50Bio UV spectrophotometer (Varian, Palo Alto, CA) equipped with a Peltier temperature controller (Quantum North-west, Spokane, WA) (*36*, *37*). Prior to any measurements, all samples were equilibrated at the initial temperature for at least 24 h. The samples were allowed to equilibrate at least 15 min until the UV absorbance was time-independent at each subsequent temperature point. Thermal transitions of samples equilibrated in quartz cells of 1 mm path length were examined by collecting data at 225 nm from 5 °C to 80 °C at 5 °C increments. Values of T_m were determined from the reflection point in the transition region (first derivative). All samples were dissolved in water at 0.50 mg/mL.

NMR Spectroscopy. NMR spectroscopy was done on a Bruker Avance DRX500 500 MHz spectrometer (Bruker, Bremen, Germany). NMR samples were prepared in H_2O/D_2O (2:3) (v/v) with a peptide concentration of about 0.10 mg/mL, stored at 4 °C for at least 24 h, and equilibrated for another 1 h at specified temperature before data acquisition. 1D NMR spectra were recorded with a spectral width of 8012.820 Hz at 15 °C.

Cell Culture. Hep3B liver cells (ATCC, Manassas, VA) were cultured in Dulbecco's modified Eagle's medium (DMEM) (Gibco, Grand Island, NY) supplemented with 10% fetal bovine serum (FBS) (Hyclon, Logan, UT), 110 mg/L sodium pyruvate (Sigma-Aldrich), 1% antimycotic solution (Sigma-Aldrich), and 1% nonessential amino acids (Sigma-Aldrich). The cells were maintained in a 75 cm^2 T-flask and incubated at 37 °C in the presence of 5% CO_2 and 95% relative humidity in an Autoflow NU-4850 CO_2 water-jacketed incubator (NuAire Inc, Plymouth, MN).

Cell Adhesion Assay. Nunclon Delta TC Microwell plates were coated with 100 μL of 50 μg/mL collagen peptides or calf-skin collagen solution at 4 °C overnight. The nonspecific binding site of the well-plate was blocked with 100 μL of 1% heat denatured bovine serum albumin (BSA) (Sigma-Aldrich) and then washed with PBS two times. A 100 μL amount of Hep3B cell suspension in serum-free DMEM (10×10^5 cells/mL) was then added and incubated for 1 h at room temperature (20 °C). The plates were washed with PBS two times to remove the unattached cells. Adhered cells were measured by a total DNA quantification assay Hoechst 33258 (Sigma-Aldrich). Briefly, the cells were lysed by freeze−thaw cycles thrice in ultrapure water, and the cell lysates were mixed with 2 μg/mL bis-benzimide in 10 mM TrisHCl (pH 7.4), 1 mM EDTA, and 0.2 M NaCl fluorescence assay buffer and were incubated in dark for 30 min. The fluorescence was read on a GENious microplate reader (Tecan, Männedorf, Switzerland) with 360 nm as excitation and 465 nm as emission. Assays were conducted in triplicate, and the data were expressed as mean ± standard deviation (SD).

Competition Inhibition Assay. Plates were coated with 100 μL of 50 μg/mL calf skin collagen solution as described above. Hep3B cells (10×10^5 cells/mL) were incubated with 50 μg/mL peptides in serum-free DMEM to saturate the cell surface receptors for 30 min before seeding. For each competition assay, a 100 μL amount of the cell suspension was seeded to the collagen-coated well, and the competitive adhesion was allowed to take place for 1 h at room temperature (20 °C). The assay was undertaken in triplicate, and the data were presented as mean ± SD. The attached cells were measured by the total DNA quantification method. The adhesion of cells in the blank serum-free medium was used as a 100% reference level.

Immunofluorescence Staining. Substrates were prepared as described above on a Lab-Tek chambered coverglass. Hep3B cells were allowed to adhere on the substrates at a density of 280 cells/mm^2 in serum-free medium for 3 h. Attached cells were fixed in cold 3.7% formaldehyde for 5 min, permeabilized in 0.1% Triton X-100 for 5 min, and blocked in blocking buffer (1% BSA in PBS) for 0.5 h. Direct immunofluorescence staining of the cell membrane-cytoskeletal vinculin with monoclonal anti-vinculin fluorescein isothiocyanate (FITC) conjugate (Sigma-Aldrich) (1:100 dilution in PBS) was allowed to proceed for 1 h. The actin cytoskeleton and cell nucleus were stained by incubating the cells with phalloidin−tetramethylrhodamine isothiocyanate (TRITC) (Sigma-Aldrich) (1:1000 dilution in PBS) for 1 h and with 4′,6-diamidino-2-phenylindole (DAPI) (Sigma-Aldrich) (1:1000 dilution in PBS) for 5 min, respectively. A Zeiss LSM510 META confocal microscope (Zeiss, Thornwood, NY) was used for imaging.

Statistical Analysis. The data of cell adhesion and competition inhibition are presented as mean ± standard deviation. The statistical analysis of the data was done using

Student's *t* test. A 95% confidence level was considered significant.

RESULTS AND DISCUSSION

Synthesis of PT-Assembled Collagen Peptides. Many protein mimics have been created by incorporating non-naturally derived chemical compounds for the template or spacer (*20*−*24*, *38*). To design a fully natural mimic, we propose a peptide template to engineer collagen mimetic that is only constituted with amino acids, consistent with native proteins. For the purpose of mimicking collagen more closely and in a more simplified manner, we have engineered a novel template composed of Gly-Phe-Gly-Glu−Glu-Gly (GFGEEG) hexapeptide that also has the unique collagen-like primary structure (Figure 1), the repeating Xxx-Yyy-Gly sequences, to assemble collagen peptides into triple-helical conformation that resembles the native structure of collagen. This peptide template (PT) has three carboxyl groups connected to the N-termini of three collagen-mimetic peptides (Figure 1).

The synthesis of template-assembled collagen peptides by solid-phase peptide synthesis poses a number of challenging problems that are usually not encountered in the stepwise synthesis of linear peptides. Ottl et al. utilized a complex and carefully planned strategy of orthogonal protection and deprotection of Cys residues to facilitate the chemoselective disulfide bridging of three cysteine-peptides (*25*, *26*). Fields et al. used a lysine−lysine-based construct furnished with aminohexanoic acid spacers to template-assemble their collagen-like sequences (*17*, *18*, *39*). Branching of three peptide strands from the lysine−lysine-based construct required three different protecting strategies: N^{α}-amino protection, N^{ϵ}-amino side chain protection which must be stable to the N^{α}-amino protecting group removal conditions, and *C*-carboxyl protection, which must be orthogonally stable to both N^{α}- and N^{ϵ}-amino protecting group removal conditions (*17*, *18*, *39*). A carefully designed branching protocol is essential to ensure the proper coupling and parallel growth of several peptide chains onto a single template and at the same time produce template-assembled collagen mimetics of high purity.

In this study, a rather simple and direct synthesis scheme based on a generally applicable Fmoc-solid-phase synthesis method, wherein no complex strategies are required, was used to synthesize a series of PT-assembled collagen peptides (Figure 2). Fmoc-GFGEEG template and collagen peptides were first synthesized separately on the resin. Subsequently, the Fmoc-GFGEEG were cleaved from the resin, activated, and coupled to NH_2-Gly_n-(Xxx-Yyy-Gly)$_n$-resin manually. To ensure optimum yield of the PT-assembled collagen peptides, Fmoc-GFGEEG was used as the limiting reagent. A cell binding motif (GFOGER) was incorporated into the PT-assembled collagen peptides, denoted as PT-CP3 and PT-CP4, to mimic collagen integrin-specific adhesion. The synthesized PT-assembled collagen peptides were harvested using mild cleavage conditions and purified. Figure S1 shows the analytical HPLC profiles of the purified PT-assembled collagen peptides and their respective MALDI-TOF MS spectra. All peptides were purified to a final purity of at least 85%. Based on the mass of the peptides obtained after HPLC purification, the yields of the PT-assembled CP1, CP2, CP3, and CP4 were approximately 2%, 8%, 9%, and 1.7%, respectively. The purified materials eluted as a single distinct peak in an analytical RP-HPLC which demonstrated the success of this synthesis protocol. The small peak shoulder may be indicative of deletion peptides of close physical properties to that of the parent molecules. However, the biophysical studies have indicated the formation of stable triple-helical conformations by the PT-assembled collagen peptides even in the presence of these deletion peptides. MALDI-TOF MS was used to verify the identity of each product, and the result showed that the molecular weight of each product obtained is consistent with that of the desired product: PT-CP1 $[M + H]^+ = 4776.4$ (calculated = 4776.5); $[M + Na]^+ = 4799.39$ (calculated = 4799.5), PT-CP2 $[M + H]^+ = 3172$ (calculated = 3172.7); $[M + Na]^+ = 3195$ (calculated = 3195.6), PT-CP3 $[M + H]^+ = 4864.1$ (calculated = 4864.04); $[M + Na]^+ = 4887.1$ (calculated = 4887.04), and PT-CP4 $[M + H]^+ = 7729.55$ (calculated = 7729.4); $[M + Na]^+ = 7752.43$ (calculated = 7752.4).

These PT-assembled collagen peptides are distinguished from other protein and collagen mimics (*14*, *15*, *17*, *18*, *20*−*22*, *24*−*26*) by the use of a peptide template that has a collagen-like primary structure and the fully amino acid-based contents, which closer mimics the structure of native collagen. The distinctive characteristics of our peptide (Figure 1b) are as follows: first, a branching peptide composed of GFGEEG used as a template to covalently link three collagen peptides to facilitate the folding of the triple helix. Second, a fully peptide-based template which allows the incorporation of other biologically active sequences at its extension for additional functions such as enzymatic cross-linking sites and integrin-specific adhesion domains. Third, the incorporation of phenylalanine in the template design as a chromophore for peptide concentration determination. Fourth, the EEG tripeptide at the C-terminus of the peptide template to provide three carboxylic arms for coupling with collagen peptides. Finally, the glycine residues which were used as spacers to reduce steric hindrance and to provide flexibility to ensure proper alignment of the three peptide strands with one-residue register shift necessary for the assembly of triple helix.

CD Spectroscopy. The collagen-like triple-helical conformation of the PT-assembled collagen peptides was verified using CD spectroscopy. Natural collagen exhibits a unique CD spectrum characterized by a large negative peak at around 197 nm, a cross-over near 213 nm, and a positive peak at approximately 220 nm (*40*, *41*). These features have been frequently used as a basis to determine the presence of synthetic collagen-like triple-helical structures in solution.

The function of the peptide template in the folding of triple-helical structures was examined by comparing the CD spectra of the PT-assembled collagen peptides with their corresponding nontemplated counterparts (CP1, CP2, CP3, and CP4). Nontemplated $(Pro\text{-}Hyp\text{-}Gly)_{10}$ was used as a stable prototype of a triple helix in this study. The PT-assembled collagen peptides and CP4 exhibited CD spectra features characteristic of collagen-like triple helix, including a positive peak around 220−225 nm and a large negative trough near 200 nm (Figure 3). These CD spectra undergo a red shift in their band positions, as compared to that of the collagen (Table S1), because of the higher percentage of imino acid content (*42*). In general, the CD spectra of PT-CP1, PT-CP2, PT-CP3, PT-CP4, and CP4 are comparable

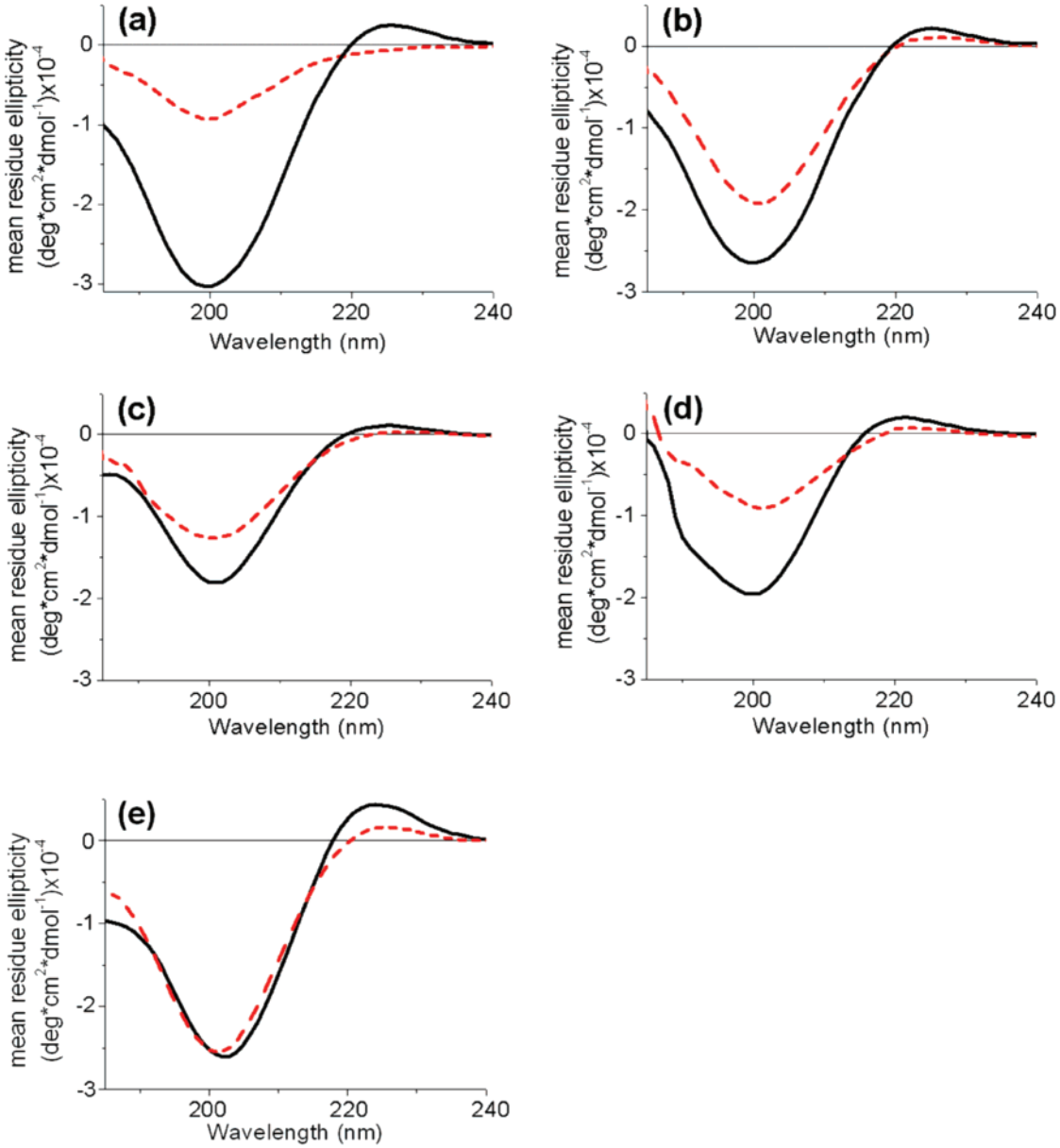

FIGURE 3: CD spectra of the PT-assembled and nontemplated collagen peptides. CD spectra of the nontemplated (a) $(Pro\text{-}Hyp\text{-}Gly)_{10}$ (solid line) and $(Pro\text{-}Pro\text{-}Gly)_3$ (segmented line) in water at room temperature. CD spectra of the PT-assembled collagen peptides (solid line): (b) PT-CP1, (c) PT-CP2, (d) PT-CP3, and (e) PT-CP4 and their nontemplated counterparts (dashed line): (b) CP1, (c) CP2, (d) CP3, and (e) CP4 in water at room temperature. $(Pro\text{-}Hyp\text{-}Gly)_{10}$ was used as a stable prototype of a triple helix while $(Pro\text{-}Pro\text{-}Gly)_3$ oligopeptide was used as a negative control.

to that of natural collagen (Figure S2) and of $(Pro\text{-}Hyp\text{-}Gly)_{10}$ (Figure 3a). The establishment of triple-helical conformations by CD spectral band positions was also supported by comaring the CD spectra of the PT-assembled collagen peptides with that of native collagen after thermal denaturation (Figure S3). At elevated temperature, a significant decrease in the intensity of both positive and negative peaks of calf-skin collagen was observed, indicating a thermal transition from the folded to unfolded state. The CD spectra of the PT-assembled collagen peptides exhibited similar trends at high temperature. However, the degree of conformational change is much smaller than that displayed by the native collagen. This is probably due to the stabilizing effect of the template. The template effect is primarily entropic. It prevents unfolding at one end of the triple-helix and thus shifted the folding/unfolding equilibrium. This observation provides evidence for the presence of the triple helices in solution.

Conversely, the nontemplated counterparts of the PT-assembled collagen peptides, except CP4, displayed CD spectra (Figure 3) of polyproline II-like structure characterized by the shallow peak at around 200 nm and the lack of the positive peak (*21*, *23*). The patterns of these CD spectra are similar to that of $(Pro\text{-}Pro\text{-}Gly)_3$ single chain peptide as given in Figure 3a, which is known to have no triple-helical conformation in solution. The result is consistent with the previous studies that short synthetic $(Pro\text{-}Hyp\text{-}Gly)_n$ cannot assume triple-helical structures in water (*21*). Increasing the chain length of repeating Pro-Hyp-Gly triplets can help to enhance the assembly of the triple-helical conformation. Alternatively, a template can be used to induce and stabilize the assembly of the triple-helical conformation for very short peptide chains (*21*, *23*). The formation of triple-helical conformation using short synthetic peptides represents an important breakthrough in the engineering of collagen

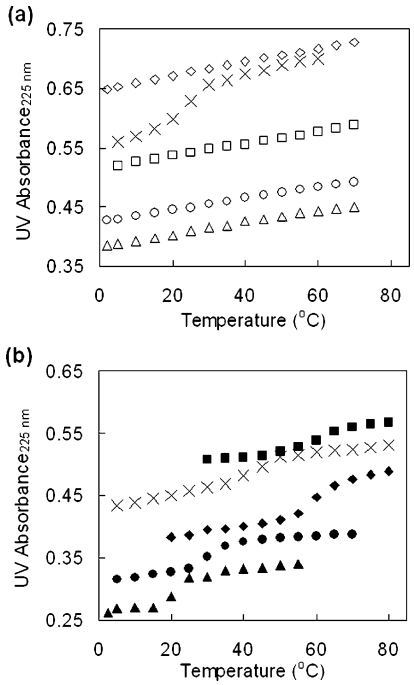

FIGURE 4: Thermal melting curve analysis. Melting transition curves of (a) nontemplated: CP1 (◊), CP2 (○), CP3 (△), CP4 (×), and (Pro-Pro-Gly)$_3$ (□) and (b) (Pro-Hyp-Gly)$_{10}$ (■), PT-assembled collagen peptides: PT-CP1 (♦), PT-CP2 (●), PT-CP3 (▲), and PT-CP4 (×) at 0.50 mg/mL in water.

analogues and preparation of collagen-mimetic biomaterials.

Rpn Values. Rpn values denote the ratio of positive peak over negative peak intensity in the CD spectra and have been previously used to establish the presence of triple-helical conformations in solution (*21*, *36*). The CD spectra absorbance and Rpn values of the PT-assembled collagen peptides and CP4, listed in Table S1, are comparable to that of calf-skin collagen for indications of triple-helical conformations. Rpn values of PT-CP4 and CP4 were 0.17 and 0.09, respectively. Higher Rpn values were obtained for PT-CP1 (0.11), PT-CP2 (0.11), and PT-CP3 (0.18) as compared to their nontemplated counterparts which have Rpn values ranging from 0.02 to 0.06. The PT-assembled collagen peptides and CP4 have Rpn values close to or higher than that of natural collagen (0.12) and the triple-helical (Pro-Hyp-Gly)$_{10}$ (0.11). These data suggest that the PT-assembled collagen peptides contain triple-helical conformations, while the nontemplated counterparts, except CP4, do not. This conclusion is also supported by the results obtained from both CD spectroscopy and thermal melting curve analyses.

Melting Curve Analyses. Triple-helical conformations can be distinguished from the polyproline II-like and non-supercoiled structures based on the thermal melting characteristic (*43*). Triple helices melt in a highly cooperative manner, as the structures are stabilized by both intra- and interstrand hydrogen-bonding water networks (*1*, *43*, *44*). Thermal denaturation of natural collagen will cause a hyperchromic effect in UV absorbance, and a similar effect can be observed for synthetic collagen-like peptides (*45*). The melting transition curves are given in Figure 4. The midpoint of the transition was taken as the melting point temperature (T_m) and is presented in Table 1.

It can be seen from Figure 4a that the nontemplated CP1, CP2, and CP3 showed similar melting curves as the negative control (Pro-Pro-Gly)$_3$ with no transition and thus no evidence of triple helicity even at low temperature. The *R* values for the four melting curves of these nontemplated collagen peptides obtained by a linear fitting are greater than 0.996, suggesting that these melting curves are a linear line with no transition. The result is consistent with the CD spectroscopy that none of the nontemplated CP1, CP2, and CP3 can assume stable triple-helical structures in water in the absence of a template since their chain length is too short to support a triple helix.

The use of the peptide template in promoting assembly of short peptide sequences into triple-helical conformations is clearly seen by the cooperative melting curves displayed by PT-CP1, PT-CP2, PT-CP3, and PT-CP4 as given in Figure 4b. While nontemplated (Pro-Hyp-Gly)$_3$ showed no transition, PT-CP2 composed of three short (Pro-Hyp-Gly)$_3$ exhibited a cooperative melting curve in water with T_m of 30 °C. The thermal stability of the PT-assembled (Pro-Hyp-Gly)$_3$ was comparable to KTA-tethered (Gly-Pro-Hyp)$_3$, which was shown to also form triple-helical conformation in water with a melting temperature of 30 °C (*22*). As the peptide chain length increases, the thermal stability of the PT-assembled conformations increases significantly as demonstrated by PT-CP1 composed of three (Pro-Hyp-Gly)$_5$ assembled by the peptide template (T_m = 59 °C). The melting temperature of nontemplated (Pro-Hyp-Gly)$_{10}$ in water is 60 °C as obtained from its melting curve given in Figure 4b, which is quite close to the T_m of PT-CP1. Therefore, it can be seen that the stabilizing effect of the peptide template is similar and equivalent to the addition of five more Pro-Hyp-Gly repeats to the nontemplated (Pro-Hyp-Gly)$_5$ chain. This result proves the significant role of the peptide template in the assembly of short collagen peptide chains into stable triple helices in solution. PT-CP3 supplemented with integrin-specific GFOGER sequence (*29*, *30*) was also found to have stable triple-helical conformation with T_m = 20 °C. The observation of a cooperative transition curve together with a proper CD spectrum is indicative of the presence of stable triple-helical conformation (*46*). It is clear that substitution of the cell binding domain into Pro-Hyp-Gly repeats may destabilize the triple helix. However, the co-oligomeric structures are still able to form triple helices.

Nuclear Magnetic Resonance Spectroscopy. The presence of the triple-helical conformation in the peptide solution can also be established by NMR spectroscopy. The assembly of a triple-helical structure results in the appearance of a new set of NMR resonances which cannot be observed for the unassembled or unfolded collagen analogues (*47*−*49*). It is remarkable that among the resonances of the assembled triple-helical set, that of Pro $C_\delta H$ at 3.1 ppm is well resolved and not overlapped by any resonance of the unfolded structure sets. The resonance at 3.1 ppm can therefore be used unambiguously to identify the triple-helical structure (*47*).

Figure 5 showed the 1D ^{1}H HMR spectral region containing the assembled Pro $C_\delta H$ resonance for collagen analogues (Pro-Hyp-Gly)$_{10}$, PT-CP1, and PT-CP2. It can be seen from Figure 5 that both (Pro-Hyp-Gly)$_{10}$ (used as a stable prototype of triple helix in this study) and PT-CP1 displayed a strong peak signal at near 3.1 ppm. This is consistent with the previous CD and UV melting curve analyses that both the collagen analogues adopt stable triple-helical conformation in solution. Also in agreement with the previous analyses,

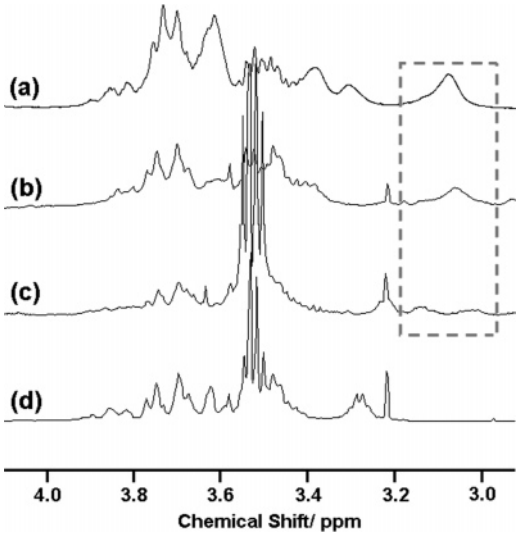

FIGURE 5: 1D ^{1}H NMR spectra of (a) $(Pro\text{-}Hyp\text{-}Gly)_{10}$, (b) PT-CP1, (c) PT-CP2, and (d) CP1. The boxed spectral regions contain a peak signal representative of the assembled Pro $C_\delta H$ signal at 3.1−3.0 ppm. All spectra were acquired at 15 °C.

PT-CP2 with lower triple helix stability showed a relatively lower peak signal with dispersion at near 3.1 ppm (Figure 5c). The result showed that three triplets are minimally sufficient to form an assembled structure. Goodman et al. proposed that the resonance dispersion is induced by the triple helix end effect and is more significant in shorter peptides (*47*). This interpretation is consistent with the wide broadening of the Pro $C_\delta H$ signal at near 3.1 ppm observed for PT-CP2 as compared to PT-CP1 and $(Pro\text{-}Hyp\text{-}Gly)_{10}$. On the other hand, it is known from our previous results that CP1 is not stable in the assembled form and therefore the set of triple-helical resonance at near 3.1 ppm is absent in CP1 (Figure 5d).

Collagen Peptide Activity. Cell adhesion assay was performed to study the cell binding activity of PT-CP3 and PT-CP4 and to understand the specific functions of the protein structure in correlation with specific amino acid sequences in the cell binding process. Collagen and heat-denatured BSA were used as a positive and negative control, respectively. The human carcinoma Hep3B cell line has a high constitutive activity in adhesion to collagen and therefore was used as the model cell type (*50*).

The cell adhesion result is presented in Figure 6a. The cell binding activity of PT-CP3 and PT-CP4 was found to be 36 ± 5% and 62 ± 1% of that of natural collagen, respectively. The presence of both PT-CP3 and CP4 promoted modest but significant adhesion of Hep3B at a similar level (∼40%). The cell adhesion can be observed to be conformation-dependent by comparing the differences in cell adhesion levels on PT-CP4, PT-CP3, CP4, and CP3. The above studies have demonstrated that while PT-CP4 adopts a stable triple-helical conformation, PT-CP3 and CP4 have lower T_m values (20 and 25 °C, respectively) and thus may undergo some degree of dissociation. Conversely, CP3 cannot assume a triple helix structure. These conformational differences resulted in a considerable loss of recognition. It is interesting to note that both PT-CP2 and CP3 promoted cell adhesion at a comparable level probably because of their similar triple helicity. The result is consistent with the fact that native collagen has a noticeably higher affinity for collagen-specific

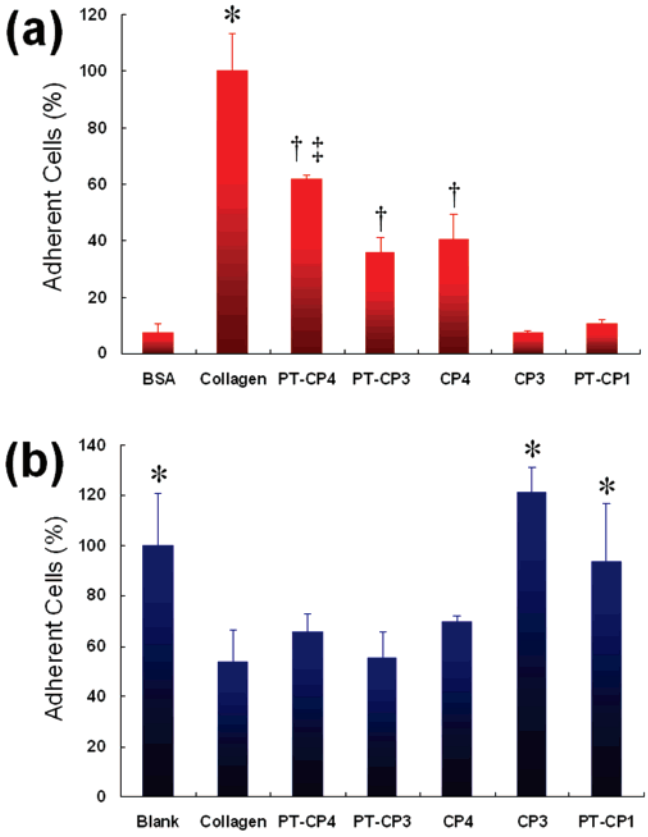

FIGURE 6: Cell adhesion and competitive adhesion. (a) Adhesion of Hep3B cells as a function of surface composition: 1% heat-denatured BSA (BSA), calf-skin collagen (collagen), PT-CP4, PT-CP3, CP4, CP3, and PT-CP1. Cells in serum-free medium were allowed to adhere to peptide- or protein-coated well plate for 1 h at 20 °C. Student's *t* test with $^*p < 0.001$: significantly different from all other samples, with $^\dagger p < 0.001$: significantly different between BSA, CP3, and PT-CP1, and with $^\ddagger p < 0.05$: significantly different from PT-CP3 and CP4. (b) Competition inhibition of Hep3B cell adhesion to collagen-coated surface. Cells in serum-free medium were incubated with 50 μg/mL peptide or collagen for 30 min prior to seeding. Cell adhesion in blank serum-free medium was used as a positive control. Student's *t* test with $^*p < 0.05$: significantly different from blank, CP3, and PT-CP1.

receptors than denatured collagen (*51*, *52*). Furthermore, the triple-helical conformation of collagen has been shown to be essential, if not crucial, for influencing cell adhesion, spreading, migration, matrix metalloproteinase (MMP) binding, and human platelet adhesion and aggregation (*16*, *30*, *31*, *53*). It has been reported that $(Gly\text{-}Pro\text{-}Hyp)_9$ and $(Gly\text{-}Pro\text{-}Pro)_{10}$ can serve as substrates for rat hepatocytes at least to some extent (*54*), suggesting that repeating tripeptide units composed of Gly and Pro might be recognized by the hepatocyte-binding sites. However, in this study, a low degree of cell attachment to the triple-helical PT-CP1, with reference to the cell adhesion of the blank (BSA) surface, was observed, which we attribute to the lower number of tripeptide repeats found in PT-CP1. PT-CP1 also lacks a GFOGER cell adhesion sequence which similarly would have an adverse effect on the level of Hep3B cell adhesion, thus indicating the specific recognition of the GFOGER sequence by cells. In all, cell recognition of collagen peptides appeared to be both conformation and sequence-specific dependent, and the absence of either resulted in a marked loss of cell adhesion. These findings may have great impact for biological chemists in their biomolecular design: shorter, and hence

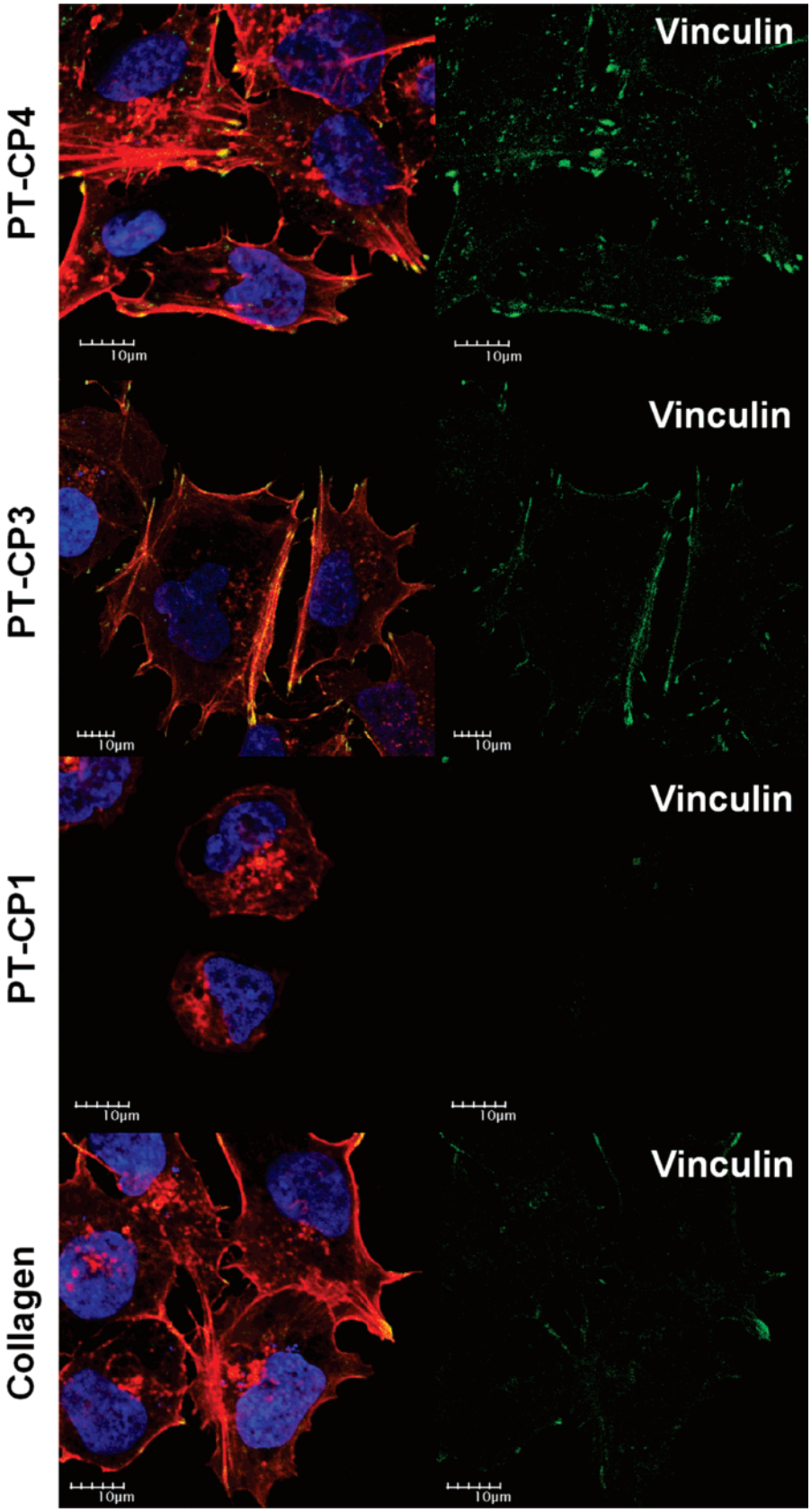

FIGURE 7: Immunofluorescence images of Hep3B cells on PT-CP4, PT-CP3, PT-CP1, and calf-skin collagen. Confocal images were taken after the cells, in serum-free medium, were seeded on different surfaces for 3 h.

less expensive, collagen peptides can be used as a stable triple-helical molecular architecture with our template assembly strategy to improve their cell recognition by supplementing them with a specific cell-binding sequence.

Hep3B cells seeded on PT-CP4, PT-CP3, PT-CP1, and collagen substrates were fixed and stained for actin stress fibers (TRITC-phalloidin; red), nuclei (DAPI; blue), and vinculin (FITC-anti-vinculin; green), a major membrane-

cytoskeletal protein present in focal adhesion plaques that is involved in the linkage of integrins to actin cytoskeleton (*55*), to study the cytoskeletal organization and focal adhesion formation. The confocal images are shown in Figure 7. It can be observed that the cells seeded on PT-CP4 and PT-CP3 exhibited collagen-like adhesion profiles, as the cells displayed distinct actin stress fibers. The assembled elongated actin filaments indicated the formation of strong actin cytoskeleton organization in the cells. Conversely, the actin organization was much less pronounced on the cells seeded on CP3 (Figure S3) and PT-CP1. Most cells remained in spherical morphology after 1- and 3-h adhesion on CP3 and PT-CP1. Deletion of the GFOGER sequence in the PT-CP1 or loss of triple helical structure in the CP3 caused a substantial decrease in cell-spreading activities.

It can be seen from the vinculin staining (Figure 7) that the cells formed strong focal adhesion contacts on both PT-CP4 and PT-CP3 surfaces. Most of the vinculin were found at the cell periphery and center, associated with the ends of stress fibers of the cells. Though the cellular recognition of GFOGER sequence cannot be measured quantitatively by immunofluorescence staining, it can be qualitatively seen from the confocal images that the cells on both PT-CP4 and PT-CP3 surfaces exhibited higher concentrations of vinculin and thus more focal contacts than the cells seeded on CP3 (Figure S3) and PT-CP1 surfaces, indicating a more firm adhesion and more rapid interaction between the cell surface receptors and GFOGER sequence. Cells did not form strong focal contacts on non-triple-helical GFOGER (CP3) and PT-CP1, as the vinculin are observed at relatively low densities at the periphery of the cells. The focal adhesion position at the convergence of integrin adhesion, signaling, and the actin cytoskeleton generally involve integral membrane protein integrins, which bind to extracellular proteins via specific amino acid sequences, such as the RGD motif. Therefore, we hypothesize that cell adhesion and spreading on collagen, PT-CP4, and PT-CP3 surfaces are unlike the interaction between the cells and synthetic polymers, which merely depends on the nonspecific contact between the cell membrane proteins and the functional groups of polymers (*56*, *57*). The extensive cell spreading could, in fact, be a result of the integrin-mediated cell adhesion process (*18*, *58*).

The competitive inhibition assay is an indirect screening for the cell binding activity displayed by the peptides. Cell adhesion to the collagen surface was inhibited when the cell surface receptors, especially specific collagen receptors, are presaturated with the adhesive molecules prior to cell seeding. The inhibitory activity of PT-CP4 and PT-CP3 was similar to that of collagen and is shown in Figure 6b. It can be seen that both PT-CP4 and PT-CP3 effectively inhibited Hep3B cell binding to collagen. The inhibition was most probably due to the specific interactions between the adhesive peptides and the cell surface receptors, suggestive of the participation of specific collagen receptors in the adhesion process. Removal of GFOGER sequence or loss of the triple helix structure resulted in collagen peptides lacking the ability to inhibit the integrin-mediated cell adhesion process. The triple-helical GFOGER appeared to represent the critical recognition for the collagen receptors.

CONCLUSION

The synthesis and biophysical studies described in this paper show that a simple strategy for making a peptide template composed of GFGEEG hexapeptide to assemble collagen-like peptide sequences into proper triple-helical molecular architecture was successfully developed. The biological assays demonstrated the successful imitation of collagen integrin-specific adhesion by the PT-assembled collagen peptide supplemented with a GFOGER sequence. Cell recognition of the collagen peptides appeared to be both conformation and sequence-specific dependent, the absence of which resulted in a marked loss of cell recognition. This peptide template assembly strategy appears to be versatile for creating and stabilizing desired collagen-like molecular architectures. Such a template-assembly system could be used to further study protein folding, to create novel protein mimetics, to insert additional specific functions into the protein mimetics by incorporating bioactive sequences at the extension of the peptide template, or to coat biomaterials to engineer integrin-specific surfaces.

SUPPORTING INFORMATION AVAILABLE

CD parameters, Rpn values, HPLC chromatograms, MALDI-TOF MS spectra of each peptide, and an immunofluorescence image of Hep3B cells seeded on CP3. This material is available free of charge via the Internet at http://pubs.acs.org.

REFERENCES

1. Bella, J., Eaton, M., Brodsky, B., and Berman, H. M. (1994) Crystal and Molecular Structure of a Collagen-Like Peptide at 1.9 Å Resolution, *Science 266*, 75−81.
2. Engel, J., and Prockop, D. J. (1991) The Zipper-like folding of collagen triple helices and the effects of mutations that disrupt the zipper, *Annu. Rev. Biophys. Biophys. Chem. 20*, 137−152.
3. Kobayashi, Y., Sakai, R., Kakiuchi, K., and Isemura, T. (1970) and Physicochemical analysis of (Pro-Pro-Gly)n with defined molecular weight-temperature dependence of molecular weight in aqueous solution, *Biopolymers 9*, 415−425.
4. Sakakibara, S., Kishida, Y., Kikuchi, Y., Sakai, R., and Kakiuchi, K. (1968) Synthesis of poly-(L-prolyl-L-prolylglycyl) of defined molecular weight, *Bull. Chem. Soc. Jpn. 41*, 1273−1275.
5. Sakakibara, S., Inouye, K., Shudo, K., Kishida, Y., Kobayashi, Y., and Prockop, D. J. (1973) Synthesis of (Pro-Hyp-Gly)n of defined molecular weights Evidence for the stabilization of collagen triple helix by hydroxypyroline, *Biochim. Biophys. Acta 303*, 198−202.
6. Engel, J., Chen, H.-T., Prockop, D. J., and Klump, H. (1977) The triple helix=coil conversion of collagen-like polytripeptides in aqueous and nonaqueous solvents. Comparison of the thermodynamic parameters and the binding of water to (L-Pro-L-Pro-Gly)n and (L-Pro-L-Hyp-Gly)n, *Biopolymers 16*, 601−622.
7. Gauba, V., and Hartgerink, J. D. (2007) Self-Assembled Heterotrimeric Collagen Triple Helices Directed through Electrostatic Interactions, *J. Am. Chem. Soc. 129*, 2683−2690.
8. Johnson, G., Jenkins, M., McLean, K. M., Griesser, H. J., Kwak, J., Goodman, M., and Steele, J. G. (2000) Peptoid-containing collagen mimetics with cell binding activity, *J. Biomed. Mater. Res. 51*, 612−624.
9. Cejas, M. A., Kinney, W. A., Chen, C., Leo, G. C., Tounge, B. A., Vinter, J. G., Joshi, P. P., and Maryanoff, B. E. (2007) Collagen-Related Peptides: Self-Assembly of Short, Single Strands into a Functional Biomaterial of Micrometer Scale, *J. Am. Chem. Soc. 129*, 2202−2203.
10. Wang, A. Y., Mo, X., Chen, C. S., and Yu, S. M. (2005) Facile Modification of Collagen Directed by Collagen Mimetic Peptides, *J. Am. Chem. Soc. 127*, 4130−4131.

11. Mo, X., An, Y., Yun, C., and Yu, S. (2006) Nanoparticle-assisted, visualization of binding interactions between collagen mimetic peptide and collagen fibers, *Angew. Chem., Int. Ed. 45*, 2267−2270.
12. Kotch, F. W., and Raines, R. T. (2006) Self-assembly of synthetic collagen triple helices, *Proc. Natl. Acad. Sci. U.S.A. 103*, 3028−3033.
13. Paramonov, S. E., Gauba, V., and Hartgerink, J. D. (2005) Synthesis of Collagen-like Peptide Polymers by Native Chemical Ligation, *Macromolecules 38*, 7555−7561.
14. Thakur, S., Vadolas, D., Germann, H. P., and Heidemann, E. (1986) Influence of different tripeptides on the stability of the collagen triple helix. II. An experimental approach with appropriate variations of a trimer model oligotripeptide, *Biopolymers 25*, 1081−1086.
15. Roth, W., and Heidemann, E. (1980) Triple helix-coil transition of covalently bridged collagenlike peptides, *Biopolymers 19*, 1909−1917.
16. Fields, G. B. (1991) A model for interstitial collagen catabolism by mammalian collagenases, *J. Theor. Biol. 153*, 585−602.
17. Fields, C. G., Lovdahl, C. M., Miles, A. J., Hageini, V. L. M., and Fields, G. B. (1993) Solid-Phase synthesis and stability of triple-helical peptides incorporating native collagen sequences, *Biopolymers 33*, 1695−1707.
18. Fields, C. G., Mickelson, D. J., Drake, S. L., McCarthy, J. B., and Fields, G. B. (1993) Melanoma cell adhesion and spreading activities of a synthetic 124- residue triple-helical "mini-collagen", *J. Biol. Chem. 268*, 14153−14160.
19. Hojo, H., Akamatsu, Y., Yamauchi, K., and Kinoshita, M. (1997) Synthesis, and structural characterization of triple-helical peptides which mimic the ligand binding site of the human macrophage scavenger receptor, *Tetrahedron 53*, 14263−14274.
20. Greiche, Y., and Heidemann, E. (1979) Collagen model peptides with antiparallel structure, *Biopolymers 18*, 2359−2361.
21. Feng, Y., Melacini, G., Taulane, J. P., and Goodman, M. (1996) Acetyl-terminated and template-assembled collagen-based polypeptides composed of Gly-Pro-Hyp sequences. 2. Synthesis and conformational analysis by CD, UV absorbance and optical rotation, *J. Am. Chem. Soc. 118*, 10351−10358.
22. Goodman, M., Feng, Y., Melacini, G., and Taulane, J. P. (1996) A Template-induced incipient collagen-like triple-helical structure, *J. Am. Chem. Soc. 118*, 5156−5157.
23. Kwak, J., Capua, A. D., Locardi, E., and Goodman, M. (2002) TREN (Tris(2-aminoethyl)amine)- An Effective Scaffold for the assembly of triple helical collagen mimetic structures, *J. Am. Chem. Soc. 124*, 14085−14091.
24. Yamazaki, S., Sakamoto, M., Suzuri, M., Doi, M., Nakazawac, T., and Kobayashi, T. (2001) Synthesis of novel all-cis-functionalized cyclopropane template assembled collagen models, *J. Chem. Soc., Perkin Trans. 1*, 1870−1875.
25. Ottl, J., and Moroder, L. (1999) Disulfide-bridged heterotrimeric collagen peptides containing the collagenase cleavage site of collagen Type, I. Synthesis and conformational properties, *J. Am. Chem. Soc. 121*, 653−661.
26. Ottl, J., Battistuta, R., Pieper, M., Tschesche, H., Bode, W., Kuhn, K., and Moroder, L. (1996) Design, and synthesis of heterotrimeric collagen peptides with a built-in cystine knot models for collagen catabolism by matrix-metalloproteases, *FEBS Lett. 398*, 31−36.
27. Ruoslahti, E., Pierschbacher, M. D. (1987) New perspectives in cell adhesion: RGD and integrins, *Science 238*, 491−497.
28. Hynes, R. O. (1990) *Fibronectins*, Springer-Verlag, New York.
29. Knight, C. G., Morton, L. F., Onley, D. J., Peachey, A. R., Messent, A. J., Smethurst, P. A., Tuckwell, D. S., Farndale, R. W., and Barnes, M. J. (1998) Identification in collagen type I of an integrin $\alpha_2\beta_1$-binding site containing an essential GER sequence, *J. Biol. Chem. 273*, 33287−33294.
30. Knight C. G., Morton L. F., Peachey A. R., Tuckwell D. S., Farndale R. W., and Barnes, M. J. (2000) The collagen-binding A-domains of integrins $\alpha_1\beta_1$ and $\alpha_2\beta_1$ recognize the same specific amino acid sequence, GFOGER, in native (triple-helical) collagens, *J. Biol. Chem. 275*, 35−40.
31. Miles, A. J., Skubitz, A. P. N., Furcht, L. T., and Fields, G. B. (1994) Promotion of cell adhesion by single-stranded and triple-helical peptide models of basement membrane collagen alpha1-(IV) 531−543, *J. Biol. Chem. 269*, 30939−30945.
32. Staatz, W., Fok, K., Zutter, M., Adams, S., Rodriguez, B., and Santoro, S. (1991) Identification of a tetrapeptide recognition sequence for the alpha 2 beta 1 integrin in collagen, *J. Biol. Chem. 266*, 7363−7367.
33. Vandenberg, P., Kern, A., Ries, A., Luckenbill-Edds, L., Mann, K., and Kühn, K. (1991) Characterization of a Type IV collagen major cell binding site with affinity to the $\alpha_1\beta_1$ and the $\alpha_2\beta_1$ integrins, *J. Cell Biol. 113*, 1475−1483.
34. Reyes, C. D., and García, A. J. (2003) Engineering integrin-specific surfaces with a triple-helical collagen-mimetic peptide, *J. Biomed. Mater. Res. 65A* (4), 511−523.
35. Reyes, C. D., and García, A. J. (2004) alpha2 beta1 integrin-specific collagen-mimetic surfaces supporting osteoblastic differentiation, *J. Biomed Mater Res. 69A* (4), 591−600.
36. Feng, Y., Melacini, G., Taulane, J. P., and Goodman, M. (1996) Collagen-based structures containing the peptoid residue Nleu-synthesis and biophysical studies of Gly-Pro-Nleu sequences by CD, UV absorbance and optical rotation, *Biopolymers 39*, 859−872.
37. Kajiyama, K., Tomiyama, T., Uchiyama, S., and Kobayashi, Y. (1995) Phase transitions of sequenced polytripeptides observed by microcalorimetry, *Chem. Phys. Lett. 247*, 299−303.
38. Mutter, M., Tuchscherer, G. G., Miller, C., Altmann, K. H., Carey, R. I., Wyss, D. F., Labhardt, A. M., and Rivier, J. E. (1992) Template-assembled synthetic proteins with four-helix-bundle topology. Total chemical synthesis and conformational studies, *J. Am. Chem. Soc. 114*, 1463−1470.
39. Fields, C. G., Grab, B., Lauer, J. L., and Fields, G. (1995) Purification and analysis of synthetic, triple-helical "minicollagens" by reversed-phase high-performance liquid chromatography, *Anal. Biochem. 231*, 57−64.
40. Brown, F. R., Corato, A. D., Lorenzi, G. P., and Blout, E. R. (1972) Synthesis and structural studies of two collagen analogues Poly (-prolyl-seryl-glycyl) and poly (-prolyl-alanyl-glycyl), *J. Mol. Biol. 63*, 85−99.
41. Sakakibara, S., Kishida, Y., Okuyama, K., Tanaka, N., Ashida, T., and Kakudo, M. (1972) Single crystals of (Pro-Pro-Gly)10, a synthetic polypeptide model of collagen, *J. Mol. Biol. 65*, 371−372.
42. Rippon, W. B., and Walton, A. G. (1971) Optical properties of the polyglycine II helix, *Biopolymers 10*, 1207−1212.
43. Jefferson, E. A., Locardi, E., and Goodman, M. (1998) Incorporation of achiral peptoid-based trimeric sequences into collagen mimetics, *J. Am. Chem. Soc. 120*, 7420−7428.
44. Bella, J., Brodsky, B., and Berman, H. M. (1995) Hydration structure of a collagen peptide, *Structure 3*, 893−906.
45. Wood, G. C. (1963) Spectral changes accompanying the thermal denaturation of collagen, *Biochem. Biophys. Res. Commun. 13*, 95−99.
46. Feng, Y., Melacini, G., and Goodman, M. (1997) Collagen-based, structures containing the peptoid residue *N*-isobutylglycine (Nleu)-synthesis and biophysial studies of Gly-Nleu-Pro sequences by CD and optical rotation, *Biochemistry 36*, 8716−8724.
47. Melacini, G., Feng, Y., and Goodman, M. (1996) Acetyl-terminated, and template-assembled collagen-based polypeptides composed of Gly-Pro-Hyp sequences. 3. conformational analysis by ^{1}H NMR and molecular modeling studies, *J. Am. Chem. Soc. 118*, 10359−10364.
48. Brodsky, B., Li, M.-H., Long, C. G., Apigo, J., and Baum, J. (1992) NMR and CD studies of triple-helical peptides, *Biopolymers 32*, 447−451.
49. Li, M., Fan, P., Brodsky, B., and Baum, J. (1993) Two-dimensional, NMR assignments and conformation of (Pro-Hyp-Gly)10 and a designed collagen triple-helical peptide, *Biochemistry 32*, 7377−7387.
50. Masumoto, A., Arao, S., and Otsuki, M. (1999) Role, of beta1 Integrins in adhesion and invasion of hepatocellular carcinoma cells, *Hepatology 29*, 68−74.
51. Santoro, S. A. (1986) Identification of a 160,000 dalton platelet membrane protein that mediates the initial divalent cation-dependent adhesion of platelets to collagen, *Cell 46*, 913−920.
52. Gullberg, D., Gehlsen, K.R., Turner, D.C., Åhlén, K., Zijenah, L. S., Barnes, M. J., and Rubin K. (1992) Analysis of $\alpha_1\beta_1$, $\alpha_2\beta_1$ and $\alpha_3\beta_1$ integrins in cell-collagen interactions: identification of conformation dependent $\alpha_1\beta_1$ binding sites in collagen type I, *EMBO J. 11*, 3865−3873.
53. Grab, B., Miles, A. J., Furcht, L. T., and Fields, G. B. (1996) Promotion of fibroblast adhesion by triple-helical peptide models of type I collagen-derived sequences, *J. Biol. Chem. 271*, 12234−12240.
54. Rubin, K., Höök, M., Öbrink, B., Timpl, R. (1981) Substrate adhesion of rat hepatocytes: mechanism of attachment to collagen substrates, *Cell 24*, 463−470.

55. Ezzell, R. M., Goldmann, W. H., Wang, N., Parasharama, N., and Ingber, D. E. (1997) Vinculin Promotes Cell Spreading by Mechanically Coupling Integrins to the Cytoskeleton, *Exp. Cell Res. 231*, 14−26.
56. Bačáková, L., Mareš, V., Bottone, M. G., Pellicciari, C., Lisá, V., and Švorčík, V. (2000) Fluorine-ion-implanted polystyrene improves growth and viability of vascular smooth muscle cells in culture, *J. Biomed Mater Res. 49*, 369−379.
57. Bačáková, L., Walachová, K., Švorčík, V., and Hnatowicz, V. (2000) Molecular mechanisms of improved adhesion and growth of an endothelial cell line cultured on polystyrene implanted with fluorine ions, *Biomaterials 21*, 1173−1179.
58. Hynes, R. O. (1992) Integrins: Versatility, modulation, and signaling in cell adhesion, *Cell 69*, 11−25.

BI702018V